Journal of Polymers and the Environment (2019) 27:364–371
https://doi.org/10.1007/s10924-018-1337-x

ORIGINAL PAPER

Effect of the Phenological Stage in the Natural Rubber Latex Properties

Natalia Trinidad Zapata-Gallego[1] · **Mónica Lucía Álvarez-Láinez**[1]

Published online: 12 December 2018
© Springer Science+Business Media, LLC, part of Springer Nature 2018

Abstract
Natural Rubber Latex (NRL) from *Hevea brasiliensis* is a material studied because of their industrial applications. For its natural origin, it is possible to find rubber particles, proteins, phospholipids and ashes. These non-rubber content are responsible for the latex colloidal stability. *H. brasiliensis* tree goes through four stages during the year, changing its nutritional requirements and as a result the rubber yield and stability. Most studies have correlated latex characteristics and yield with tree age and clonal origin but none of them with phenological stages. The impact of the phenological stage on the material properties has not been completely identified yet. In this work, the influence of the clonal origin and the phenological stage with the material properties is studied. Thermal behavior, microstructural analysis, morphological study, colloidal stability and rheology are analyzed for FX3864, IAN710 and AIN873 clones during 1 year. NRL is an amorphous material but during the high-yield period, a melting point is observed. Flowering is the stage when phospholipids, protein and isoelectric point are higher. Phenological stages do not affect the rubber, but the main changes are in the non-rubber content.

Keywords Rubber latex · Phenological stages · Non-rubber content · Colloidal stability · Rheology

Introduction

Tires are usually produced of synthetic rubber with 55% of world rubber demand. Furthermore, manufacturing activity growth will demand rubber for non-tire applications and also, it is expected that natural rubber will remain crucial in products like surgical gloves, mattress, balloons and condoms, due to its remarkable elasticity.

Natural Rubber Latex (NRL) from *Hevea brasiliensis* is a colloidal dispersion containing 30–40% rubber particles (*cis*-1,4-polyisoprene), 5% non-rubber particles (proteins, phospholipids among others) and < 1% in inorganic compounds. It is well known that *cis*-1,4-polyisoprene molecule has α- and ω-terminal groups, that interact whit the phospholipids and proteins phase respectively, dissolved in the serum [1, 2]. This phospholipid-protein content is related with the ability to enhance the colloidal stability of NRL and the rubber properties after curing [3].

✉ Mónica Lucía Álvarez-Láinez
malvar26@eafit.edu.co

[1] Department of Product Design Engineering, Universidad Eafit, Carrera 47 sur #35-75, Medellín 050001, Antioquia, Colombia

The clone variety is extensive and new clones more resistant to climate changes and plagues are developed constantly. In Asia, RRIM 105 and RRIM 600 [4] are the most spread and cultivated clones of natural rubber. RRIM 600 is a secondary clone from *H. brasiliensis* species, a crossbreed between TJIR and PB 86 clones developed in the Rubber Research Institute of Malaysia (RRIM) [5–7]. This clone starts tapping after 5½ years, not too much foliage but a stable latex yielding with dry rubber content (DRC) average of 32.9% [8]. Since Asia/Pacific region is the biggest market for rubber products, RRIM 600 is one of the most studied species from *H. brasiliensis*. For some *H. brasiliensis* species created to resist Latin-American climate and plagues, such as FX3864, IAN873 and IAN710, no studies about how NRL components change with the phenological stages.

Besides the clone variety, rubber trees are controlled by periodically repeated cyclical changes, depending on the climate conditions; those periods are better known as phenological stages, as follows: flowering, fruit growth or filling fruit, foliation and defoliation or leaf unfolding. The studies related with phenological stage are focused in solid rubber not in latex [5]. Works related with NRL usually studied its biocompatibility with human tissues [9], as well as the comparison of properties between *H. brasiliensis* and others

Content courtesy of Springer Nature, terms of use apply. Rights reserved.

sources like *Hancornia speciosa Gomes* [10] and *Euphorbia characias* [11], and mechanical properties of UV vulcanized membranes [12].

A common problem of rubber phenological studies is not to consider the effect of tapping on tree physiology and phenological behavior, as well as the lack of correlation between the rubber yield and quality of the latex extracted. Most studies have correlated latex characteristics and yield with tree age but none of them with phenological stages. As a consequence, the impact of the phenological stage on the properties of the material has not been completely identified yet [5, 10, 13–16]. The aim of this work is to analyze the effect on the physical and chemical properties of FX 3864, IAN 710 and IAN 873 clones, driven by the phenological state.

Experimental

Materials

Freshly tapped latex was obtained from three different clones: FX 3864, IAN710 and IAN 873. All these trees are located in an experimental area with geographic coordinates of 7°43′7″, 7°43′0″N between 75°30′26″, 75°30′16″W, with elevation 120 m a.s.l, the land is mainly flat and the soil is classified as Ultisol, Paleudults family with a higher acid pH. According to the classification system of Holdridge, the climate zone is a tropical wet forest.

All the samples were collected during a year, according to phenological phases of *H. brasiliensis* tree: starting in flowering stage from March to May; it continues with the filling fruits stage from June to August, following by foliation stage (leaf growing) from September to November and finishing with leaf unfolding stage during November to February. Each tree was labeled and the tapping system was the same (1/2S d/2).

Latex started to be collected during flowering stage. It was tapped 135 FX 3864 trees, 179 IAN 710 trees and 209 IAN 873 trees and stabilized in situ with low ammonium solution. The samples for each clone were carefully homogenized, and stored in a sunlight free atmosphere at 5–10 °C. All the analyses were carried out in the next 15 days.

Characterization

Rubber Yielding Periods

In order to identify the latex yielding through phenological changes, DRC was measured. DRC was carried out by means of Eq. (1) according to ASTM D1076. 2.0% of acid acetic solution was added to 10.0 ± 0.1 g of latex with 25.0% of total solid content (TSC) until the coagulation. This solid was laminated until reach 1 mm thick, and washed with enough water. This thin sheet was dried at 70 °C for 16 h.

$$DRC = \frac{dry\ \ coagulated\ mass}{latex\ mass} \times 100 \quad (1)$$

TSC was quantified with the Eq. (2) according to ASTM D1076. Rubber mass was obtained drying 2.5 ± 0.1 g of latex at 100 °C in an oven with circulating air for 2 h.

$$TSC = \frac{dry\ \ rubber\ mass}{latex\ mass} \times 100 \quad (2)$$

Each test was repeated three times, under controlled atmospheric temperature and relative humidity (23 °C and 60%) with 95% confidence limit.

Thermal Analysis

Differential scanning calorimetry (DSC) was used to analyze the thermal transitions for all lattices using a DSC Q200 from TA Instruments. All experiments were set up in three cycles: heating from 25 °C to 200 °C at 20 °C/min, cooling cycle from 200 °C until − 90 °C at 20 C/min; a second heating was performed in modulated mode up to 200 °C, with an amplitude of 1.27 °C every 60 s. The weight of the samples was 20 ± 1 mg.

Microstructural Analysis

A Spectrum Two FTIR–ATR from Perkin Elmer was used to identify the characteristic functional groups in films of dry rubber. The background registration and samples ATR spectra were performed with 32 scans at 1 cm^{-1} resolution from 400 to 4000 cm^{-1}. For each sample, the spectra were recorded and the mean spectrum is presented with the baseline subtracted. Protein and phospholipids content was determined by the proposed Rolere and coworkers' method [17].

Colloidal Stability

The latex stability was analyzed by means of Z potential, measured in a *Zetasizer* Ver. 6.34 by *Malvern*. The latex was diluted until 10% TSC with distilled water and solutions with pH from 4 to 12 were prepared. A drop of this solution was added to 20 ml of buffer solution. Each test was repeated two times with 95% confidence limit.

Latex Morphology

The shape and size distribution of the different lattices was studied using two different techniques: atomic force microscopy (AFM) and diffraction light scattering (DLS). AFM images were obtained with a nanosurf Easyscan2 model. It

Content courtesy of Springer Nature, terms of use apply. Rights reserved.

was used the tapping mode in air, using an integrated silicon tip/cantilever having a resonance frequency < 1 kHz and spring constant of 1 N/m. The samples were prepared using a dip coating process and in order to obtain repeatable results, different regions of the specimens were scanned. Images analysis were used to calculate the samples size distribution.

All DLS measurements were performed with a Malvern Instrument *Zetasizer* Ver. 6.34 by *Malvern* equipped with a He–Ne laser (λ = 633 nm, max 4 mW) and operated at a scattering angle of 173°. In all measurements, 1 ml of latex solution was employed and placed in a 10 mm × 10 mm quartz cuvette. The latex solution used was 0.01% of rubber content and sonicated with the aim to dissolve any aggregations.

Latex Rheology

A rheological analysis was carried out using a Haake Mars III from Thermo scientific equipped with DIN coaxial cylinders geometry with large gap; inner cylinder was a titanium rotor with radium = 10.0 ± 0.002 mm and length 30.0 ± 0.003 mm; the outer cylinder was a steel cup with radium = 10.850 mm, and the volume of the sample was 8.2 ml. Tests were carried out at room temperature in a shear rate range from 10 to 1500 s^{-1}. All measure samples were evaluated at 0.35% TSC. Each test was repeated two times, under controlled atmospheric temperature and relative humidity (23 °C and 60%) with 95% confidence limit.

Results and Discussion

The yielding pattern clones are disclosed in Fig. 1 as DRC; it shows a clear delineation between high and low yielding production. For all the clones, during flowering and filling fruit stages DRC is stable, but an abrupt change is presented during foliation (low-yielding period) and leaf unfolding (high-yielding period). According to the meteorological station data, during leaf-unfolding period the temperatures were higher and total leaf unfolding was expected, however; conform with visual inspection, leaf unfolding was partial and some mature leaves remained in the rubber tree, this behavior suggest that DRC increases, because there is no-competition of photoassimilates compounds and latex is regenerated through accumulation [18, 19].

In agreement with thermal results, the poly-isoprene compounds are the same in all the phenological stages, because the Tg values are the same in all samples, the coefficient of variation is < 1% (Fig. 2). However, for all the clones during the leaf unfolding phase the rubber particles exhibit a melting point near − 1 °C. Some authors attribute this rubber crystallization to several factors: high *cis*-1,4 isoprene unit content, long average sequence length *cis*-1,4 isoprene units, phospholipids content, gel fraction and so on [20–23]. In our

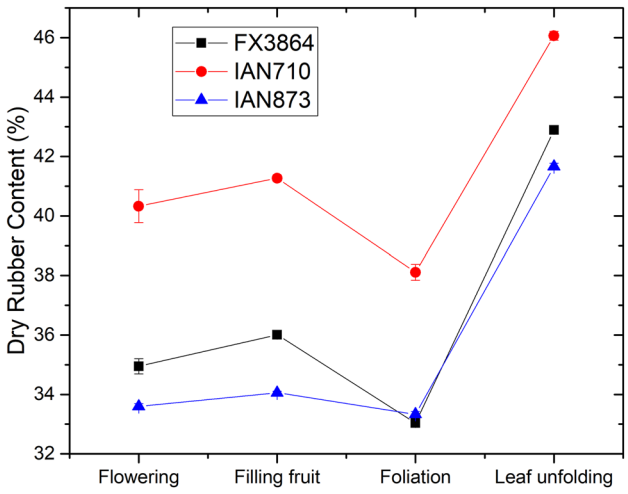

Fig. 1 Dry rubber yield as a function of phenological stage for the clones under study

case, this melting behavior is associated with the high-yield stage, so these results are correlated with the high *cis*-1,4 isoprene unit content.

In terms of FTIR results (Fig. 3), the characteristics peaks for *cis*-1,4-polyisoprene were presented in all the samples, bands between 3100 and 2725 cm^{-1} (peaks #2–6) were attributed to C–C and C–H bonds and also a peak in 840 cm^{-1} appears, which is the C–H out of plane bending band of the *cis*-1,4 addition. All these bands are the same in all clones with no changes between the phenological stages. The protein domain is described for three major bands: amine (3282 cm^{-1}, peak #1), amide I (1630 cm^{-1}, peak #9) and amide II (1541 cm^{-1}, peak #10). The phospholipids domain is defined with ester band (1747–1732 cm^{-1}, peak #7) and carboxyl band (1700 cm^{-1}, peak #8).

Protein and phospholipids content was determined by the proposed Rolere and coworkers' method [17] and presented in Fig. 4. FTIR spectra were normalized using the maximum absorbance 840 cm^{-1} (C–H out-of-plane bending). According to this method, proteins content is higher in amide I than amide II. FX3864 reduce protein content with the stages, for IAN710 is higher in foliation stage and IAN873 exhibit an almost stable protein content during the stages. Phospholipids seem to be more stable than proteins in filling fruit, foliation and leaf unfolding stages, but an abrupt increase is displayed during the flowering stage, especially for ester compounds. FX3864 exhibited the highest phospholipids content followed by IAN873. During the flowering stage, the tree is using carbohydrate reserves for flowers development, this could explain why this is a low-yield period but the non-rubber content is higher.

NRL have suspended particles coated with a thinner layer distributed with phospholipids and proteins [3, 24]. This develops, in the particle surface, a positive charge

Content courtesy of Springer Nature, terms of use apply. Rights reserved.

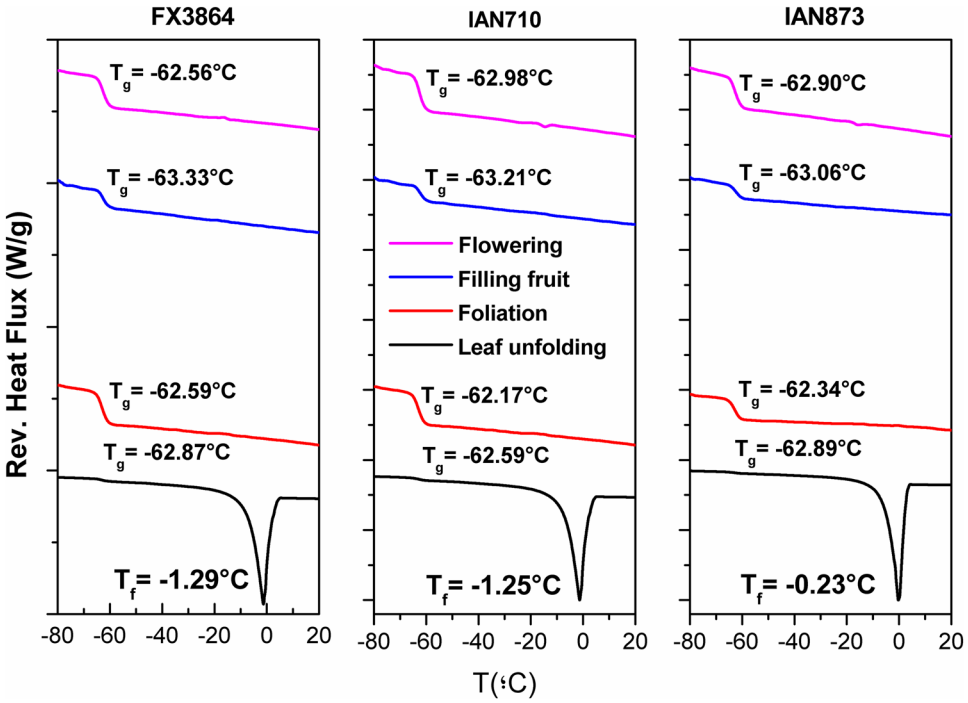

Fig. 2 FX3864, IAN710 and IAN873 thermal analysis, Tg does not change with the phenological stage

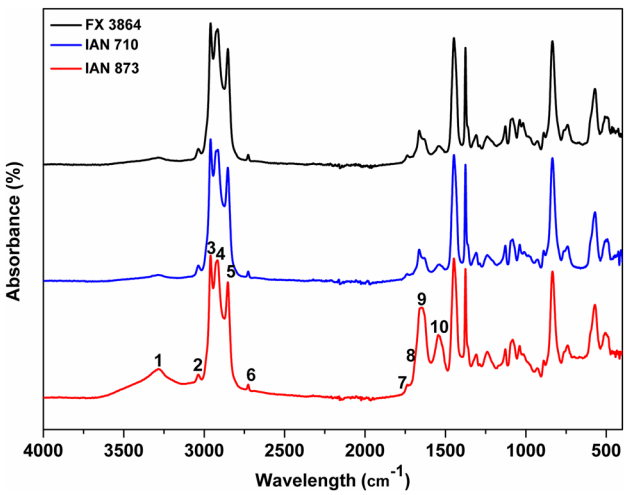

Fig. 3 FTIR spectra of FX3864, IAN710 and IAN873 clones during flowering stage. Numbers are related with NRL functional group

(generated from amino groups of the adsorbed proteins) and a negative charge (ionization of the adsorbed carboxylic group on phospholipids molecules). This arrangement is responsible of the colloidal stability in latex suspensions [3]. Figure 5 presents the Z potential value as a function of pH. In all cases, these values are negative, due to the negative charges of the proteins and carboxylic groups coating the rubber surface. Maximum stability point occurs at pH 9. For pH 10, 11 and 12 the zeta potential increases (less negative value) because of the cation absorption on the surface.

The isoelectric point is the pH value where zeta potential is zero and as a consequence, the latex losses its stability and coagulated spontaneously. In Fig. 6, it is observed this value in a narrow range between 4.0 and 3.5. A higher value in flowering stage means that the system can be more easily destabilized, as a consequence of the higher protein and phospholipids content.

In Fig. 7 is presented the particle size distribution according to AFM image analysis. FX3864 and IAN873 have a monomodal distribution with an average size around 600 nm without significant changes during a year. However, IAN710 exhibits a bimodal distribution (except in foliation) with changes in average size in all the stages. Average sizes are from 300 nm until 3 µm in all the lattices. In AFM-phase images is observed rounds and pears shape particles with dark and bright colors on the surface; these colors are related with differences in chemical composition on the rubber particles (rubber and non-rubber content) [16]. However, under the test conditions, it was not possible to find a correspondence between color and chemical composition. With the aim to compare this results, it was used a scattering technique; in Fig. 8 is disclosed the particle size distribution by DLS analysis. The particle size distribution by DLS is wider and appear a bimodal distribution in almost all the lattices with fine size around 200 nm and coarse size around 1000 nm. Differences are related with sample preparation, in AFM analysis, the samples are a dried thin film over a substrate, while in DLS the rubber particles are suspended and hydrated; this can generate a slight increase in mean size because particle surface is solvated with water.

Content courtesy of Springer Nature, terms of use apply. Rights reserved.

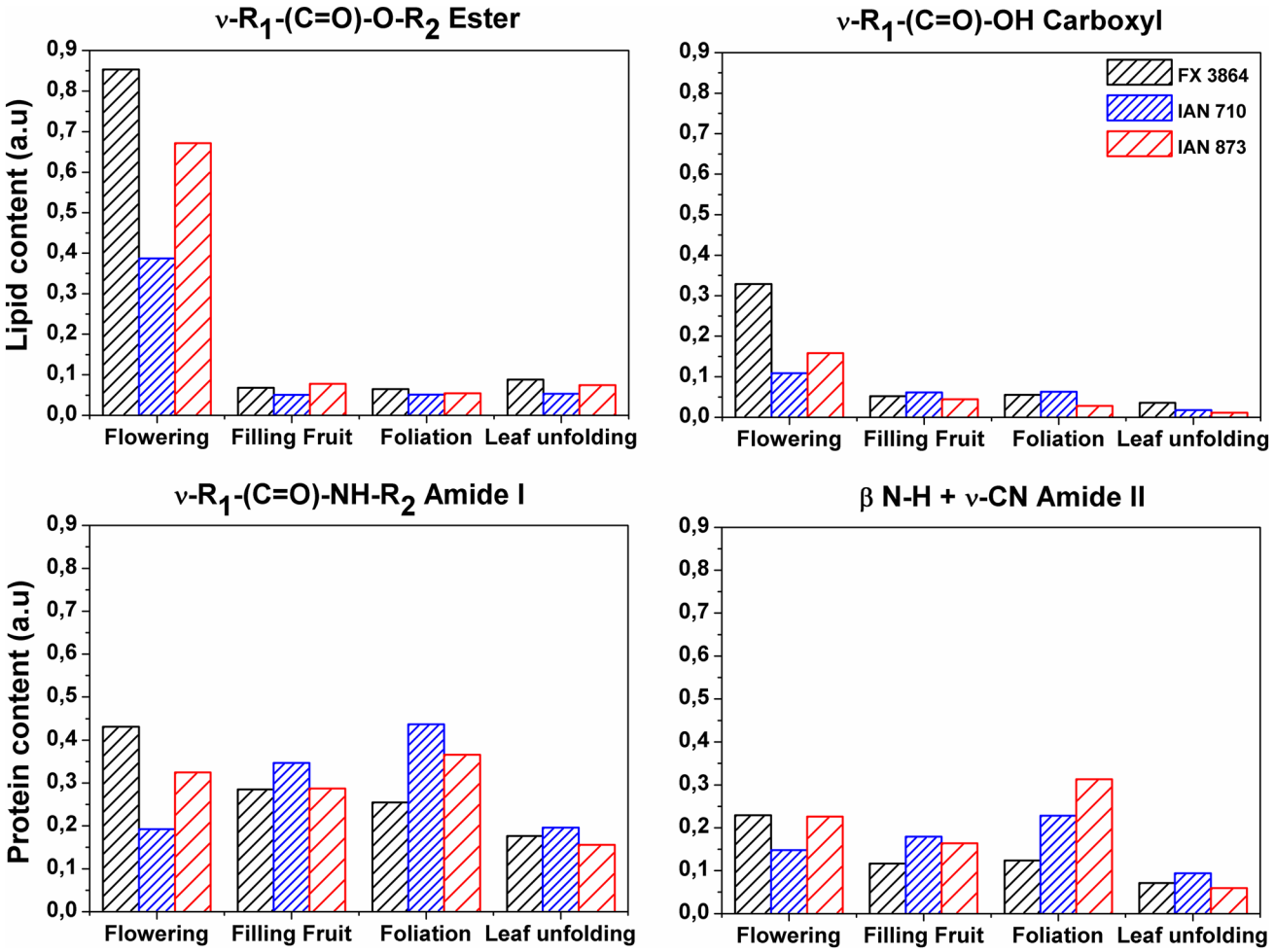

Fig. 4 Phospholipid and protein content calculated with FTIR spectra according to Rolere and coworkers' method. Upper graphs are ester and carboxyl group and lower graphs are amide I and II groups for FX3864, IAN710 and IAN873 clones

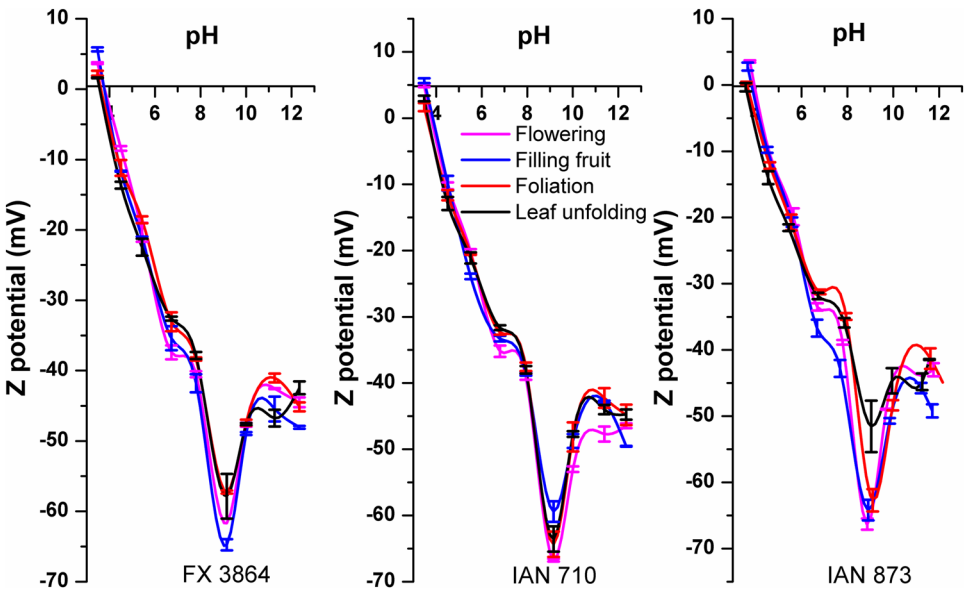

Fig. 5 Z potential as a function of pH and phenological stage for clones under study. Colloidal stability at pH 9

Content courtesy of Springer Nature, terms of use apply. Rights reserved.

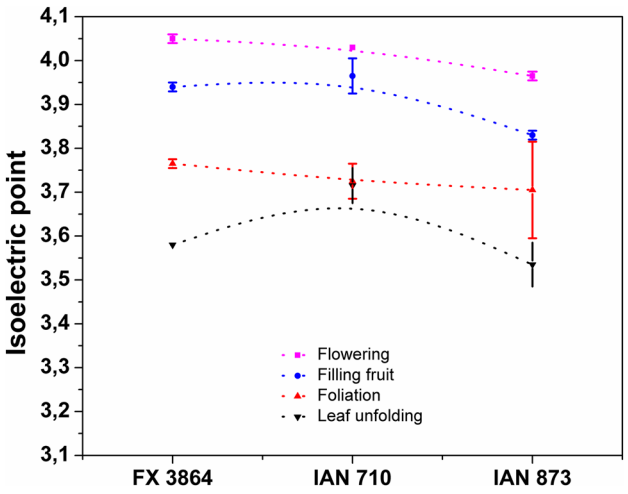

Fig. 6 Isoelectric point variations as a colloidal instability for the clones under study

Rheology in latices is related to phospholipids–protein content and therefore, with the colloidal stability. For a lower shear rate, the latex viscosity decreases to reach a minimum point, in which the viscosity starts to increase (Fig. 9). This behavior is due to differences arrangements in the latices particles. In lower shear rate, the particles form a bidimensional structure oriented in the flow direction and viscosity decreases. When shear rate exceeds a minimum viscosity, those bidimensional structures are perturbed and required more energy to establish a new arrangement in equilibrium and as a consequence the viscosity increases [25]. FX3864 shows higher viscosity in the flowering stage, this increase is related with the phospholipids content, because the higher amount of that component increases the resistance of the system to flow and more energy is required to destabilize it by means of mechanical effect. IAN873 viscosity is also higher in flowering, but in IAN710 is higher in foliation stage (higher protein content).

Conclusions

Our DSC and FTIR–ATR results suggest that *cis*-1,4-polyisoprene is the same in all the clones without a change during a year. However, it is observed differences in the chemical environment as a consequence of the phenological stage; these changes are related to the phospholipids–proteins phase. Rubber particles are amorphous, but in our case, a melting peak appears at lower temperatures (− 1 °C), this peak is associated with the high-yield stage, so these results are correlated with the high *cis*-1,4 isoprene unit content.

A comparison between scattering technique like DLS and image analysis by mean of AFM micrographs disclosed differences related to sample preparation. Being more accurate by AFM image analysis. We found more differences in size related to the type of clone rather than the phenological stage. AFM mean particle size is ~ 600 nm, while DLS mean particle size is ~ 200 nm (fine particles) and ~ 1000 nm (coarse particles).

Colloidal instability is in pH 3.5–4.0 and slightly changes with the phenological stages; it is necessary to reach pH 9.0 to stabilize the latex. Higher values of phospholipids–protein content mean that the system can

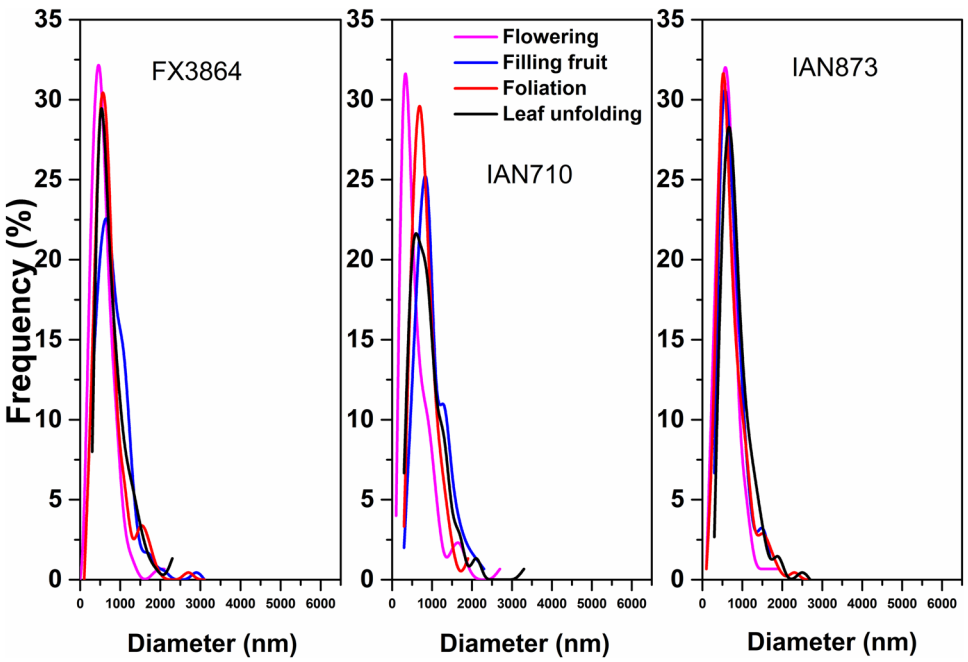

Fig. 7 Frequency as a function of particle diameter according to AFM image analysis

Content courtesy of Springer Nature, terms of use apply. Rights reserved.

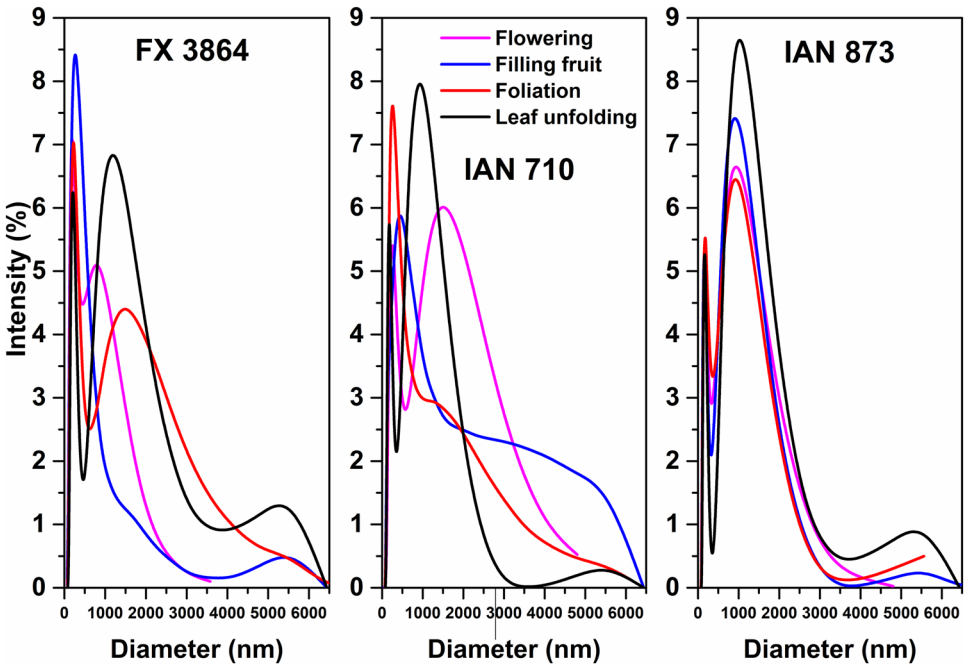

Fig. 8 DLS intensity as a function of particle diameter

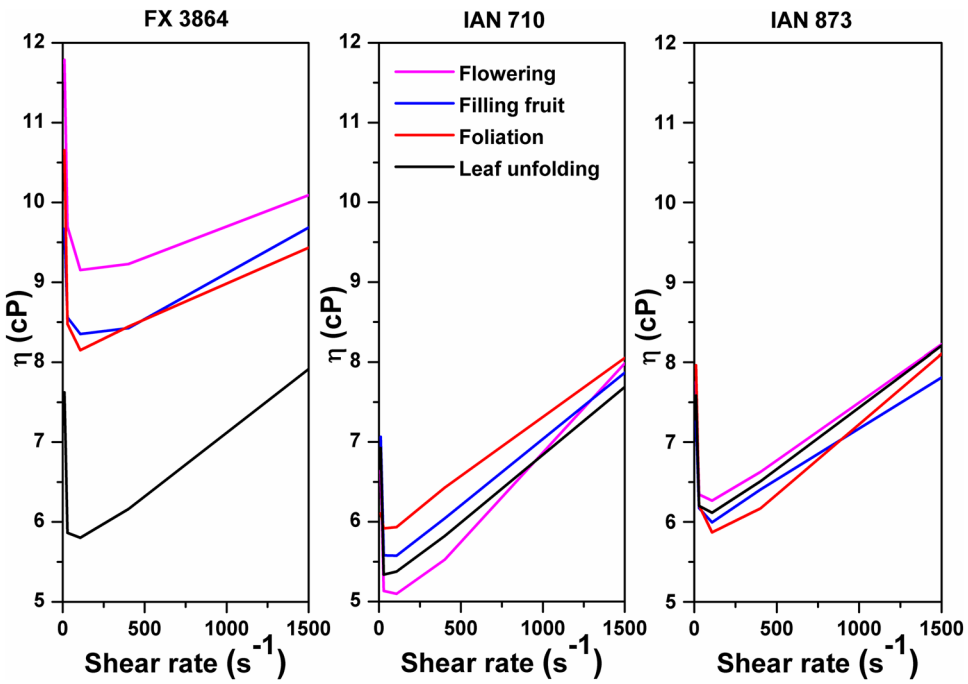

Fig. 9 Rheology curve for FX3864, IAN710 and IAN873 clones and its behavior according the phenological stage

be more easily destabilized spontaneously, but the interparticle forces (electrostatic, Van der Walls and London forces, and also steric interactions) are a key factor in the rheology behavior because they increase the resistance to flow. As a result of all these, there are attraction and repulsion interactions in the particles and the viscosity changes. The clone more dependent with the phenological stages is FX3864, while IAN873 is the more stable clone.

Acknowledgements The authors like to acknowledge the financial support from Eafit University, Royalties General Program of Colombia (Programa General de Regalías) and all the institutions involved in this project under the contract number 4600001081-2013.

Content courtesy of Springer Nature, terms of use apply. Rights reserved.

References

1. Tuampoemsab S (2008) Control of the degradation of natural rubber: analysis and application of naturally occurring anti-and pro-oxidants in natural rubber, Mahidol University
2. Tarachiwin L, Sakdapipanich J, Ute K et al (2005) Structural characterization of α-terminal group of natural rubber. 1. Decomposition of branch-points by lipase and phosphatase treatments. Biomacromolecules 6:1851
3. Sansatsadeekul J, Sakdapipanich J, Rojruthai P (2011) Characterization of associated proteins and phospholipids in natural rubber latex. J Biosci Bioeng 111:628
4. Krisnan B et al (2015) Growth assessment of popular clones of natural rubber (*Hevea brasiliensis*) under warm dry climatic conditions of chattisgarh state, central India. J Exp Biol Agric Sci 3:157
5. Silva JQ, Scaloppi Júnior EJ, Moreno RMB et al (2012) Producción y propiedades químicas del caucho en clones de Hevea según los estados fenológicos. Pesqui Agropecu Bras 47:1066
6. Rahman AYA, Usharraj AO, Misra BB et al (2013) Draft genome sequence of the rubber tree *Hevea brasiliensis*. BMC Genom 14:75
7. Gonçalves PDS, Scaloppi Júnior EJ, Martins MA et al (2011) Assessment of growth and yield performance of rubber tree clones of the IAC 500 series. Pesqui Agropecu Bras 46:1643
8. Azabache L (2012) Proyecto de factibilidad para la producción de caucho natural (*Hevea Brasiliensis*) en el Municipio de Puerto Carreño Vichada, pp 1–87
9. Floriano JF, Da Mota LSLS, Furtado EL et al (2014) Biocompatibility studies of natural rubber latex from different tree clones and collection methods. J Mater Sci Mater Med 25:461
10. Malmonge JA, Camillo EC, Moreno RMB, Mattoso LHC, McMahan CM (2009) Comparative study on the technological properties of latex and natural rubber from *Hancornia speciosa Gomes* and *Hevea brasiliensis*. J Appl Polym Sci 111:2986
11. Spanò D, Pintus F, Mascia C et al (2012) Extraction and characterization of a natural rubber from *Euphorbia characias* latex. Biopolymers 97:589
12. Haque ME, Dafader NC, Akhtar F, Ahmad MU (1995) Influence of the variation of latex clone on the mechanical properties of the radiation vulcanized natural rubber latex film. Radiat Phys Chem Oxf Engl 46:119
13. De Oliveira L, De Rosa D, De Arruda E et al (2004) Comparative studies of latex obtained of rubber tree clones (*Hevea brasiliensis*) - series IAC 328 - Votuporanga - sp. J Therm Anal Calorim 75:495
14. Quesada-Méndez I, Aristizábal-Gutiérrez F, Montoya-Castaño D (2012) Caracterización de dos parámetros del látex de clones de *Hevea brasiliensis* (Willd. ex A. Juss.) Müll. Arg. en la altillanura Colombiana. Colomb For 15:139
15. Moreno RMB, Ferreira M, Gonçalves PDS, Mattoso LHC (2005) Technological properties of latex and natural rubber of *Hevea brasiliensis* clones. Sci Agric 62:122
16. Sakdapipanich J, Kalah R, Nimpaiboon A, Ho CC (2015) Influence of mixed layer of proteins and phospholipids on the unique film formation behavior of Hevea natural rubber latex. Colloids Surf A 466:100
17. Rolere S, Liengprayoon S, Vaysse L, Sainte-Beuve J:Bonfils F (2015) Investigating natural rubber composition with Fourier transform infrared (FT-IR) spectroscopy: a rapid and non-destructive method to determine both protein and lipid contents simultaneously. Polym Test 43:83
18. Ortolani AA, Sentelhas PC, Camargo MBP, Pezzopane JEM, Gonçalves PDS (1998) Agrometeorological model for seasonal rubber tree yield. Indian J Nat Rubber Res 11:8
19. Priyadarshan P (2011) Biology of Hevea rubber. CABI, Massachusetts
20. Kawahara S et al (2000) Crystallization behavior and strength of natural rubber: skim rubber, deproteinized natural rubber, and pale crepe. J Appl Polym Sci 78:1510
21. Hamdan S, Muhamad M, Hassan J (2000) Thermal analysis of natural rubber *Hevea Brasiliensis* latex. J Rubber Res 3:25
22. Kawahara S, Takano K, Yunyongwattanakorn J et al (2004) Crystal nucleation and growth of natural rubber purified by deproteinization and trans-esterification. J Polym 36:361
23. Tarachiwin L, Sakdapipanich JT, Tanaka Y (2003) Gel formation in natural rubber latex: 2. Effect of magnesium ion. Rubber Chem Technol 76:1185
24. Nawamawat K, Sakdapipanich JT, Ho CC et al (2011) Surface nanostructure of *Hevea brasiliensis* natural rubber latex particles. Colloids Surf A 390:157
25. Khandal RK, Tadros TF (1988) Application of viscoelastic measurements to the investigation of the swelling of sodium montmorillonite suspensions. J Colloid Interface Sci 125:122

Content courtesy of Springer Nature, terms of use apply. Rights reserved.

Terms and Conditions

Springer Nature journal content, brought to you courtesy of Springer Nature Customer Service Center GmbH (“Springer Nature”).
Springer Nature supports a reasonable amount of sharing of research papers by authors, subscribers and authorised users (“Users”), for small-scale personal, non-commercial use provided that all copyright, trade and service marks and other proprietary notices are maintained. By accessing, sharing, receiving or otherwise using the Springer Nature journal content you agree to these terms of use (“Terms”). For these purposes, Springer Nature considers academic use (by researchers and students) to be non-commercial.
These Terms are supplementary and will apply in addition to any applicable website terms and conditions, a relevant site licence or a personal subscription. These Terms will prevail over any conflict or ambiguity with regards to the relevant terms, a site licence or a personal subscription (to the extent of the conflict or ambiguity only). For Creative Commons-licensed articles, the terms of the Creative Commons license used will apply.
We collect and use personal data to provide access to the Springer Nature journal content. We may also use these personal data internally within ResearchGate and Springer Nature and as agreed share it, in an anonymised way, for purposes of tracking, analysis and reporting. We will not otherwise disclose your personal data outside the ResearchGate or the Springer Nature group of companies unless we have your permission as detailed in the Privacy Policy.
While Users may use the Springer Nature journal content for small scale, personal non-commercial use, it is important to note that Users may not:

1. use such content for the purpose of providing other users with access on a regular or large scale basis or as a means to circumvent access control;
2. use such content where to do so would be considered a criminal or statutory offence in any jurisdiction, or gives rise to civil liability, or is otherwise unlawful;
3. falsely or misleadingly imply or suggest endorsement, approval , sponsorship, or association unless explicitly agreed to by Springer Nature in writing;
4. use bots or other automated methods to access the content or redirect messages
5. override any security feature or exclusionary protocol; or
6. share the content in order to create substitute for Springer Nature products or services or a systematic database of Springer Nature journal content.

In line with the restriction against commercial use, Springer Nature does not permit the creation of a product or service that creates revenue, royalties, rent or income from our content or its inclusion as part of a paid for service or for other commercial gain. Springer Nature journal content cannot be used for inter-library loans and librarians may not upload Springer Nature journal content on a large scale into their, or any other, institutional repository.
These terms of use are reviewed regularly and may be amended at any time. Springer Nature is not obligated to publish any information or content on this website and may remove it or features or functionality at our sole discretion, at any time with or without notice. Springer Nature may revoke this licence to you at any time and remove access to any copies of the Springer Nature journal content which have been saved.
To the fullest extent permitted by law, Springer Nature makes no warranties, representations or guarantees to Users, either express or implied with respect to the Springer nature journal content and all parties disclaim and waive any implied warranties or warranties imposed by law, including merchantability or fitness for any particular purpose.
Please note that these rights do not automatically extend to content, data or other material published by Springer Nature that may be licensed from third parties.
If you would like to use or distribute our Springer Nature journal content to a wider audience or on a regular basis or in any other manner not expressly permitted by these Terms, please contact Springer Nature at

onlineservice@springernature.com